MEASUREMENTS OF THE MAGNETIC FIELDS IN INTERPLANETARY SPACE AND THE MAGNETOSPHERE

Norman F. Ness
Laboratory for Space Sciences
NASA-Goddard Space Flight Center
Greenbelt, Md. USA

August 1965

Table of Contents

ABSTRACT

16051

Direct measurements of magnetic fields in space have been performed by satellites and space probes since 1958. The results of these experiments reveal the continual confinement of the geomagnetic field by the "solar wind", forming the magnetosphere and the Earth's magnetic tail. At 3-6 R_e permanent effects due to "ring currents" have been detected. Enclosing the magnetosphere is a turbulent boundary layer separated from the interplanetary medium by a collisionless MHD shock wave. At the subsolar point the distance to the termination of the regular geomagnetic field is approximately 10 R_e and to the shock wave, 13.4 R_e. The geomagnetic tail is observed out to a distance of 40 R_e trailing away from the Sun much in the fashion of cometary tails. The magnetized solar plasma contains a field of approximately 5 gammas which is directed along the classical Archimedean spiral predicted by Parker. The interplanetary field, deduced conclusively to be of solar orgin, is structured into 4 sectors which are readily identifiable during the quite years of the solar cycle (1963-64). This review summarizes the experiments and their results with respect to our knowledge of fields in space.

Author

Introduction

The advent of the satellite and space probe era 8 years ago introduced into the realm of extra-terrestrial physics the possibility of measuring directly the properties of interplanetary space unaffected by the presence of the earth. Since 1957 an impressive sequence of developments in the conduct of such in-situ experiments has led not only to renewed investigations of well known solar-terrestrial physical problems, but also initiated studies investigating completely new phenomenon not previously anticipated.

This review is directed towards a brief summary of those satellite experiments measuring magnetic fields in space and their results. These measurements include data obtained from close orbiting earth satellites at elevations of only 200 kilometers to space probes penetrating to within 0.7 A.U. (astronomical unit) and out to 1.5 A.U. from the Sun.

Interpretation of data obtained from magnetic field experiments, although frequently of and by itself is possible, either directly or indirectly incorporates the effects of the motion of charged particles. Indeed the present state of the outermost field lines for both the geomagnetic and other planetary fields as well as the interplanetary magnetic field is dominated by the solar corpuscular flux referred to as the "solar wind". We shall not review in this paper the pertinent data concerning the direct measurements of the interplanetary plasma nor the theory as so effectively and completely developed by Parker in his many publications since the late 1950's (summarized in Parker, 1963).

As a direct result of the flux of low energy plasma from the sun and the effects of its interaction with the geomagnetic field, it is logically consistent to consider dividing extra-terrestrial space into three regions:

1. The interplanetary region where the properties of the interplanetary medium are undisturbed by the presence of the earth, and its magnetic field,
2. The "magnetosheath", associated with the interaction of the solar wind with the geomagnetic field and
3. The magnetosphere, that region of space containing the geomagnetic field and encompassing the earth in the classical concept of the Chapman-Ferraro geomagnetic cavity.

Separating these three regions of space are two surfaces whose physical characteristics only recently have been investigated:

1. The collisionless magnetohydrodynamic shock wave surface separating the undisturbed interplanetary medium from the magnetosheath and
2. The magnetopause, separating the interaction region from the magnetosphere.

This review is organized to discuss firstly the magnetosphere, then the general interaction problem leading to the development of the geomagnetic "tail" and finally a discussion of the interplanetary magnetic field and the structure of the interplanetary medium.

A summary of all satellites and space probes which have carried magnetometers for the explicit purpose of measuring fields in space is given in Figures 1-5. Those experiments which have yielded mainly data on the geomagnetic field are listed in Figures 1 and 2 along with their pertinent spacecraft orbital characteristics. The experiment parameters of these satellites and space probes is given in Figures 3 and 4. Those experiments providing data principally on the interplanetary magnetic field are listed in Figure 5. There are no duplicate listings so that a single earth orbiting satellite such as Explorer XVIII (or IMP-1) which yielded data on all three regions of space appears once. The same is true of the planetary probes Mariners II and IV which yielded interplanetary data as well as the first measurements of the magnetic fields of Venus and Mars.

The Magnetosphere and its Boundary

More than 30 years ago in a study of the phenomenon of the geomagnetic storm Chapman and Ferraro, based upon an initial suggestion by Lindemann, postulated the transient ejection of solar plasma (reviewed by Chapman, 1963). This would confine the geomagnetic field temporarily and led to the development of electrical currents on the boundary whose magnetic fields represented the disturbance field observed terrestrially. Following the early suggestions of Biermann (1951) for a continuous and substantial solar corpuscular flux to explain the observed characteristics of Type-I comet tails, Parker developed the theory of the solar wind and thus concluded that a continual confinement of the geomagnetic field would exist.

Four years ago at the 1961 meeting of this conference in Kyoto, Japan the first experimental evidence of both plasma and magnetic field experiments for the confinement of the geomagnetic field and observations of the boundary were presented (Bridge et. al., 1962; Heppner et. al., 1962). Although earlier measurements on the Pioneers I and V (Sonett, 1960; Sonett et. al., 1960 a,c; Coleman et. al., 1960b; Coleman, 1964) suggested termination of the geomagnetic field, no continuous traversal of the boundary was achieved because of intermittent satellite data transmission. The Explorer X satellite (Heppner et. al., 1963; Bonetti et. al., 1963) was launched March 25, 1961 and transmitted useful information on plasma fluxes and magnetic field to apogee of its first orbit, 46.1 R_e (Earth radii). These data revealed the large scale distortion of the geomagnetic field on the nighttime side of the earth and revealed an intimate relationship between the flow of plasma and the strength of the magnetic field. As is frequently the case with such new data the initial interpretations were rudimentary and subsequent investigations of the combined set of data were necessary before a clear picture emerged as to the nature of the experimental results in the magnetosheath (Axford, 1962, Kellogg, 1962; Rossi, 1963).

Early detailed mapping of the geomagnetic field close to the earth on the Explorer VI satellite (Smith et.al., 1960; Sonett et.al., 1960b) in 1959 yield data initially interpreted to be representative of large scale permanent "ring currents" encircling the earth. Subsequent to the Explorer X results, the Explorer VI data were re-examined and shown to be consistent with a general distortion of the geomagnetic field as indicated by the Explorer X results and later satellite measurements (Smith, 1962; Smith et.al., 1964). Lunik 1 and 2 measurements between 3-6 R_e detected large depressions of the main field at 2.8-4R_e (Dolginov et.al., 1960, 1961). Recently Electron 2 (Dolginov et.al., 1965) has confirmed in the same region of space similar but weaker "ring current" effects.

The first measurements of trapped particles, fields and plasmas at the boundary of the geomagnetic field, the magnetopause, were conducted also in 1961 by Explorer XIV (Cahill and Amazeen, 1963; Freeman et.al., 1963). These data, shown in Figure 6, indicated a termination of the compressed geomagnetic field at a distance of approximately 8.2 R_e on the sun-lit side of the earth coincident with a termination of the trapping region of energetic particles as well as the onset of thermalized solar plasma. These measurements and their interpretation, combined with the Explorer X data, established the permanent existence of a confined geomagnetic field. It was also possible, at that time, with the direct measurements of the boundaries of the geomagnetic field, to place in the proper perspective the earlier measurements by the Pioneer and Explorer satellites and space probes. Interesting and substantive reviews of these early data have been provided by Obayashi (1963) and Cahill (1964).

In a study of the interaction of the solar wind with the geomagnetic field it has been appropriate to introduce a geocentric co-ordinate system which reflects the solar origin of the plasma. Direct measurements of the interplanetary plasma by Mariner II and IMP-I have indicated velocities of approximately 300 to 700 km/sec (Snyder and Neugebauer, 1962; Bridge et. al., 1965). Thus the aberration of solar plasma flow from the Sun-Earth line is only 3-6 degrees since the heliocentric orbital velocity of the Earth is 30 km/sec. The solar ecliptic co-ordinate system shown in Figure 7 has been a useful reference system in which to study measurements of fields, particles and plasma data within the magnetosphere, at its boundary and beyond.

Detailed repetitive measurements of the magnetosphere boundary were first performed by the Explorer XII satellite in 1961 and both field and particle measurements have been reported upon (Cahill and Amazeen, 1963; Freeman, 1964). A similar situation has been true of the Explorer XIV satellite in which extensive measurements of both particle (Frank, 1965) and field phenomenon (Cahill, 1964a; Cahill, 1965) have been performed and reported on recently.

A comprehensive survey with respect to direct measurements of the confined geomagnetic field, its boundary and significantly the first magnetic measurements of the collisionless shock wave have been performed by the IMP-I satellite. (Ness et.al., 1964; 1965). In figure 8 is shown the results on outbound orbit No. 1 at a solar ecliptic longitude of $\phi = 315^{\circ}$. The magnitude of the field is observed to be about that theoretically predicted by extrapolation from surface measurements. Al 11.3 R_e, the magnetopause, an abrupt decrease occurs in the magnitude of the field and the directional characteristics are best described as turbulent and disordered. This persists to 16.8 R_e or at the shock wave where the average magnitude of the field drops to approximately 5 gammas. The diagram is labeled to indicate clearly the identifiable positions of these boundaries separating the three regions of space previously defined. An important feature of these data is that in addition to the individual data points representing the magnetic field magnitude and direction, there is included the root-mean-square deviation over a 5.46 minute time interval. This measures essentially the high frequency component of the magnetic field and is particularly diagnostic in identification of the position of the collisionless shock wave. In this figure it is seen that the deviations in the individual components are well above the noise level of the instrumentation and telemetry system until a geocentric distance of 16.8 R_e is reached. This characteristic behavior of the magnetic field on the IMP-I satellite and as indicated earlier by Explorers XII and XIV was repeated for 42 times while the satellite apogee precessed from close to the subsolar point to the midnight meridian plane.

In addition to the conspicious features observable in the magnetic field data, during each traversal of the interaction region, is the corresponding plasma data obtained by the MIT group (Bridge et. al., 1965). The corresponding data for outbound orbit No. 1. from their publication is shown in Figure 9. An estimate of the isotropy of flow of plasma during each spacecraft rotation is made by recording the maximum and minimum fluxes. Clearly indicated in these results is the nearly isotropic flux observed in a region of space which corresponds almost perfectly with the results of the magnetic field experiment in defining the interaction region as containing a disordered magnetic field. On the basis of a classical gas dynamic analogy Kellogg (1962) and others have shown that a detached bow shock wave should develop surrounding the compressed geomagnetic field since the flow of solar plasma is supersonic in the Alfvén magnetohydrodynamic sense at a Mach number of 5-10.

A direct comparison of the results obtained with both the magnetic field and plasma experiments on the IMP-I satellite has revealed the identification of both boundaries at approximately the same points along the trajectory to within a fraction of an earth radius.

Theoretical computations of the shape of the magnetosphere boundary have been conducted by a number of authors (reviewed by Beard, 1964). In addition to computing the shape of the magnetosphere, Spreiter and Jones (1963) computed the shape of the detached bow shock wave which would be expected on the basis of the gas dynamic model previously suggested. A direct comparision with the theoretically predicted shape and position of the shock is shown in Figure 10. The crosses represent magnetosphere boundary traversals, the dots the collisionless shock and the agreement is seen to be quite good. A slight adjustment of the theoretical standoff ratio for the shock wave has been necessary in order to bring the observations into good harmony with the theory. At the present time detailed studies of the mechanisms leading to the development of a collisionless shock wave with specific application to the case of the solar wind interaction with the geomagnetic field are being conducted by a number of separate individuals (Corday, 1965; Noerdlinger, 1964). Although the details do not appear to be theoretically well understood, the observational evidence is strong to indicate the existence of the shock wave although certain authors, notably Bernstein, et. al., 1964; Fredericks et. al., 1965 and Scarf et. al., 1965, contend that actually only a broad disordered region is present.

At the present time there is strong controversy between the plasma measurements obtained on the IMP-I and II satellites relating to the observed turbulent isotropic plasma flow within the transition region and near the stagnation point. Work by Wolfe et. al. (1965) on IMP-II has reported an opposite point of view in that the plasma flow is still from the Sun. This discrepancy in the experimental results has yet to be resolved although it is difficult to understand those results of Wolfe et. al. (1965) which indicate plasma flow with a large velocity component normal to the magnetosphere boundary within the magnetosheath.

The Earth's Magnetic Tail

The first measurements of the earth's magnetic field at great distances from the earth were performed by the Explorer X satellite in 1961. These results indicated the distortion of the geomagnetic field so that the lines of force were observed to trail out far behind the earth pointing roughly away from the earth. Subsequently Explorer XIV (Cahill 1964 a, 1965) revealed that near local midnight the terrestrial field appeared to approach predominately an anti-solar direction at 16 R_e. Recent detailed measurements mapping the earth's magnetic tail have been performed by the IMP-I satellite (Ness, 1965b) and have shown that the geomagnetic field trails out far behind the earth at least halfway to the moon and forms a "magnetic tail". That such an appendage to the geomagnetic field would exist was anticipated in the theoretical work of Parker (1958), Piddington (1960), and most recently and definitively by Axford, Petschek and Siscoe (1965), Dessler (1964), Dessler and Juday (1965).

Detailed measurements from orbit No. 41 of the IMP-I satellite present in Figure 11 that orbit closest to the midnight meridian plane. The results are presented in a solar ecliptic coordinate system and demonstrate the remarkable feature of the field observations indicating a decided orientation parallel to the earth-sun line and directed either towards or away from the sun depending upon whether or not the satellite is above or below a magnetically neutral region identified as a neutral sheet. The work of Axford et. al., (1965) pointed out the necessity for the existence of an enhanced plasma flux within the neutral sheet region. This was previously measured by the Explorer XIV satellite in the work of Frank (1965), Frank and Van Allen (1964) in which an energetic particle "tail" was observed. Lunik 2 data by Gringauz (1960) was interpreted as being evidence for a 3rd radiation belt although as Van Allen (1964) noted, the importance of interpreting such data in terms of the solar wind distortion of the geomagnetic field and the day-night assymetry cannot be neglected.

A remarkable feature of the detailed results on the nightside of the earth, represented by Figure 11 has been the observed development of the distorted geomagnetic field in which field lines from the polar cap regions are dragged out to form the magnetic tail. A summary of these observations is presented in Figure 12 showing the projection of the XY solar ecliptic components of the magnetic field in the earth's magnetic tail as viewed on the plane of the ecliptic. Figure 12 shows the results obtained when above or below an imaginary plane at $Y_{se} = -2.5\ R_e$ chosen for clarity of presentation. In these presentations it is possible to identify the traversal of the neutral sheet on each orbit and in some cases each orbit traverses the neutral sheet more than once. This is interpretable in view of the "wobble" of the earth's magnetic dipole once every 24 hours and the associated orientation of the magnetic neutral sheet.

A summary of the magnetic field topology within the magnetosphere as observed in the magnetic mid-night meridian plane is shown in Figure 13.

Included also for reference are the distorted field lines containing of the terrestrial radiation belts showing the significant day-night assymetry which is a direct result of the impact of the solar wind and the development of the earth's magnetic tail. Recently Williams and Mead (1965) and Ness and Williams (1965) have shown that the motion of particles observed in the radiation belts exhibit a day-night assymetry which can be correlated with the existence and temporal behavior of the magnetic field in the earth's magnetic tail. This lends strong support to this overall field topology since the motion of charged particles in the radiation "trap" clearly integrates the overall disturbance fields due to the confinement of the geomagnetic field.

Recent measurements were conducted of the planet Mars by the Mariner IV spacecraft indicating essentially no magnetic field for that planet. It has been previously reported from the Mariner II results (Smith et.al., 1965) that Venus may have only a small field. On the basis of IMP-I, only a turbulent wake of the moon in the flow of solar wind (Ness, 1965 a) was detected. Lunik 2 data (Dolginov et.al., 1961 b) detected no significant lunar field. Thus it appears that the study of the interaction of various planetary objects with the solar wind and the development of a magnetic tail depends upon whether or not the object possesses an inherent magnetic field. In the case of the earth a large magnetic tail develops and a similar phenomenon may be expected to development behind the planet Jupiter since all indications are that it possesses an appreciable magnetic field trapping particles originating in the interaction of the solar wind with its magnetic field. Trailing downstream in the solar wind flow from such objects as the Moon, Mars and Venus are possibly only turbulent wakes.

Interplanetary Magnetic Field

The existence, general description and temporal behavior of the interplanetary magnetic field have been deduced in the past from a variety of terrestrial observations, notably the analysis of energetic particle trajectories impacting the earth. The analysis by McCraken (1962) is indicative of recent efforts which indicate the preferential guiding of solar particles to the Earth from West limb flare events when compared to East limb events. This strongly suggests the development of the Archimedean spiral structure in the interplanetary magnetic field which is the direct result of the continuous solar wind flux. Direct measurements in space by Pioneer V (Coleman et.al., 1960a) with a search coil magnetometer were the first performed and revealed a magnetized solar plasma with a magnetic field deduced initially to be mainly normal to the ecliptic plane. Recent work to analyze the Pioneer V data by Greenstadt (1965) has yielded results differing with the earlier analyses and shows that the fields measured are much closer to the plane of the ecliptic with a magnitude of 5 to 10 gammas. Measurements of the interplanetary magnetic field by Explorer X (Heppner et.al., 1963) were distorted by the strong interaction between the streaming plasma and the magnetic field of the earth. The magnetometer measurements on the Mariner II space probe are incomplete because of unknown spacecraft magnetic fields and do not provide accurate vector data on the interplanetary magnetic field (Smith, 1964) The data are consistent with the interplanetary field in the plane of the ecliptic with the strength of approximately 5 gammas normal to the Sun satellite direction.

Accurate measurements of the interplanetary magnetic field in Cis-lunar space have been performed on the IMP-I satellite. A sample of the data obtained is shown in Figure 14 for two 24 hour time intervals in solar ecliptic co-ordinates. Throughout most of the data the field is seen to be approximately between 4-7 gammas and to be pointed roughly away from the Sun or towards the sun at the theoretical angle associated with the Archimedean spiral structure. The directional histogram of all of the interplanetary magnetic field measurements is shown in Figure 15. Here two time intervals are chosen for the data representation, 5.46 minutes being the basic telemetry unit and 3 hours being the standard unit of time for studying various terrestrial disturbances. It is clear that the magnetic field direction preferentially parallels the plane of the ecliptic and approximately along the spiral angle in a sense either away from or towards the sun; directions referenced as positive or negative respectively.

Corresponding to the directional histogram are the magnitude histograms for the same data, shown in Figure 16. It is seen that the average magnetic field is approximately 5 gammas which corresponds to a field of two gauss at the photospheric surface of the Sun using Parker's model for the expansion of the solar corona into interplanetary space. The important question which arises in connection with the study of the magnetic field in interplanetary space is its origin and its time characteristics. A more quantitative approach to the investigation of the origin of the interplanetary magnetic field has been conducted by Ness and Wilcox (1964). The direction of the interplanetary magnetic field was assigned over each 12 hour interval to be either positive or negative depending upon the statistical preference for the direction as defined by the directional histogram shown in Figure 15. An auto-correlation function was constructed for the interplanetary magnetic field data which would indicate the tendency of the direction of the magnetic field to recur periodically. This is shown in Figure 17, indicating a strong recurrence tendency at an interval of 27 days which corresponds to the rotation period of the solar equatorial region and suggests a solar origin to the interplanetary field.

Since the interplanetary magnetic field direction at 1.A.U. appears to be periodic or recurrent with a 27 day period it is then logical to consider a direct correlation between the direction of the magnetic field observed at the surface of the sun with that observed at 1 A.U.. A cross correlation function constructed for the IMP-I data yields the result (Ness and Wilcox, 1964) that the time offset for a coherent peak is 4.5 days as shown in Figure 17 . This leads to an average plasma velocity of approximately 385 km/sec which is close to the average velocity of 312 km/sec reported by the MIT plasma experiment (Lyon, 1965) on IMP-I for the same interval of time.

Quasi Stationary Sector Structure

The most recent result of the study of the interplanetary magnetic field yet reported is the detection of an organized sectoring of the interplanetary magnetic field by the IMP-I data. (Ness and Wilcox, 1965). A circular superposed epoch chart of the direction of the interplanetary magnetic field is shown in Figure 18. It is immediately evident that the direction of the magnetic field is highly organized on a 27 day basis into four segments or sectors within each of which the direction of the field is either positive or negative most of the time. Three sectors are 7.7 days long and one is 3.8 days.

With the identification of the sector structure in the interplanetary magnetic field direction, Wilcox and Ness (1965) investigated the variation of the interplanetary magnetic field magnitude and other parameters of the interplanetary medium. Figure 19 presents the superposed epoch analysis of the magnitude of the magnetic field in three large sectors of the quasi-stationary structure. Included also is a superposed epoch analysis of the 24 hour sum Kp index corresponding to the same time interval. It is seen that during these three solar rotations there is a coherent variation of the interplanetary magnetic field strength with the planetary magnetic index Kp within each sector region.

Equally important is the variation of the interplanetary solar plasma characteristics during the sector structure. Figure 20 presents the superposed epoch analysis of both the flux and density of the solar plasma as measured by the MIT group (Lyon , 1965). It is seen that there is a similar variation of the flux and density throughout the sector structure which can be interpreted on the basis of the "frozen-in" flux concept introduced by Alfven in his study of magnetohydrodynamics. At the present time the full significance of this sector structure has yet to be investigated.

Wilcox and Ness (1965) have suggested that this sector structure may be an important aspect of the development of M-region type storms which have yet to be identified with any unique feature on the surface of the Sun. The more critical analysis of solar magnetographs in the future and their correlation with direct measurements in the interplanetary medium may provide additional data on the permanence of this sectoring of the interplanetary medium. It should be noted that as this structure rotates, temporal variations associated with it are interpreted as related to the co-rotation of the structure rather than radial propagation from the Sun.

Acknowledgements

It is my pleasure to acknowledge the important participation in the research reported upon here of my colleagues; Dr. John Wilcox of the University of California, Berkeley and Mr. Clell Scearce and Mr. Joseph Seek of the Goddard Space Flight Center. I also appreciate the opportunity to incorporate the IMP-I plasma data in these analyses prior to their publication by the MIT group.

References

Axford, W. I., 1962, J. Geophys. Res. 67, 3791.

Axford, W. I., H. E. Petschek and G. L. Siscoe, 1965, J. Geophys. Res. 70, 1231.

Beard, D. B., 1964, Rev. Geophys. 2 , 335.

Bernstein, W., R. W. Fredricks and F. L. Scarf, 1964, J. Geophys. Res. 69, 1201

Biermann, L., 1951, Z. Astrophys. 29, 274.

Bonetti, A., H. S. Bridge, A. J. Lazarus, B. Rossi and F. Scherb, 1963, J. Geophys. Res. 68, 4017.

Bridge, H. S., C. Dilworth, A. J. Lazarus, E. F. Lyon, B. Rossi and F. Scherb, 1962, J. Phys. Soc. Japan 17, A-II, 553.

Bridge, H.S., A. Egidi, A. Lazarus, E. Lyon and L. Jacobson, 1965, Space Research V, 969 .

Cahill, L. J., 1964a, I G Bulletin 79, 231.

Cahill, L. J., 1964b, in Space Physics ed. by D. P. LeGalley and A. Rosen, John Wiley and Sons, New York, 301.

Cahill, L. J., 1965, Space Research VI, to appear.

Cahill, L. J. and P. G. Amazeen, 1963 J. Goephys. Res. 68, 1835.

Chapman, S. 1963, in The Earth's Environment ed. by C. Dewitt et.al., Gordon and Breach, New York, 371.

Coleman, P. J. Jr, 1964, J. Geophys. Res 69, 3051.

Coleman, P. J.. Jr., L. Davis and C. P. Sonett, 1960a, Phys. Rev. Letters 5, 43.

Coleman, P. J., Jr., C. P. Sonett, D. L. Judge and E. J. Smith, 1960b, J. Geophys. Res. 65, 1856.

Corday, J. G., 1965, J. Geophys. Res. 70, 1278.

Dessler, A. J., 1964, J. Geophys. Res. 69, 3913.

Dessler, A. J., and R. D. Juday, 1965, Planet. Space Sci. 13, 63.

Dolginov, S. Sh., Ye. G. Yeroshenko, L. N. Zhuzgov, and L. O. Tyurmina, 1960, Space Research I, 863.

Dolginov, S. Sh., Ye. G. Yeroshenko, L. N. Zhuzgov, N. V. Pushkov and L. O. Tyurmina, 1961a, Art. Earth Sat. 3, 4, 5, 490.

Dolginov, Sh. Sh., Ye. G. Yeroshenko, L. N. Zhuzgov, N. V. Pushkov and L. O. Tyurmina, 1961b, Geomag. and Aero. 1, 21.

Dolginov, Sh. Sh., Ye. G. Yeroshenko and L. N. Zhuzgov, 1965, Space Research VI, to appear.

Frank, L. A., 1965, J. Geophys. Res. 70, 1593.

Frank, L. A. and J. A. Van Allen, 1964, in Research in Geophysics I, MIT Press, Cambridge, Mass, 161.

Fredricks, R. W., F. L. Scarf and W. Bernstein, 1965, J. Geophys Res. 70, 21.

Freeman, J. W., 1964, J. Geophys. Res. 69, 1691.

Freeman, J. W., J. A. Van Allen and L. J. Cahill, 1963, J. Geophys. Res. 68, 2121.

Greenstadt, E. W., 1965, TRW Report 9890-6001-RU000

Gringauz, K. I., V. G. Kurt, V. I. Moroz, and I. S. Shklovsky, 1960, Astron. Zh. 37-4, 716.

Heppner, J. P., N. F. Ness, T. L. Skillman and C. S. Scearce, 1962, J. Phys. Soc. Japan 17, A-II, 546.

Heppner, J. P., N. F. Ness, T. L. Skillman and C. S. Scearce, 1963, J. Geophys. Res. 68, 1.

Kellogg, P. J., 1962, J. Geophys. Res. 67, 3805.

Lyon, E. F., 1965, Private communication.

McCracken, K. G., 1962, J. Geophys. Res. 67, 447.

Ness, N.F., 1965a, J. Geophys. Res 70, 517.

Ness, N.F., 1965b, J. Geophys. Res. 70, 2989.

Ness, N. F., C. S. Scearce and J. B. Seek, 1964, J. Geophys. Res. 69, 3531.

Ness, N.F., C. S. Scearce, J. B. Seek and J. M. Wilcox, 1965, Space Research VI, to appear.

Ness, N. F., and J. M. Wilcox, 1964, Phys. Rev. Letters, 13, 461.

Ness, N. F., and J. M. Wilcox, 1965, Science 148, 1592.

Ness, N.F. and J. M. Wilcox, 1966, Ap. J., to appear.

Ness, N.F. and D. J. Williams, 1965, GSFC Report X-612-65-285

Noerdlinger, P. D., 1964, J. Geophys. Res. 69, 369.

Obayashi, T., 1964, J. Geophys. Res. 69, 861.

Parker, E. N., 1958, Phys. Fluids 1, 171.

Parker, E. N., 1963, Interplanetary Dynamical Processes, Interscience, New York.

Piddington, J. H., 1960, J. Geophys. Res. 65, 93.

Rossi, B., 1963, Space Research III, 529.

Scarf, F. L., W. Bernstein and R. W. Fredricks, 1965, J. Geophys. Res. 70, 9.

Smith, E.J., 1962 J. Geophys. Res. 67, 2045.

Smith, E. J., 1964, in Space Physics ed. by D P. LeGalley and A. Rosen, John Wiley and Sons, New York, 350.

Smith, E. J.,, P. J. Coleman, D. L. Judge and C. P. Sonett, 1960, J. Geophys. Res. 65, 1858.

Smith, E.J., L. Davis Jr., P. J. Coleman Jr. and C. P. Sonett, 1965, J. Geophys. Res. 70, 1571.

Smith, E. J., C. P. Sonett and J. W. Dungey, 1964, J. Geophys. Res. 69, 2669.

Snyder, C.W. and M. Neugebauer, 1964, Space Research IV, 89.

Sonett, C. P., 1960, Phys. Rev. Letters 5, 46.

Sonett, C. P., D.L. Judge, A. R. Sims and J. M. Kelso, 1960a, J. Geophys. Res. 65, 55.

Sonett, C.P., E.J. Smith, D. L. Judge and P. J. Coleman, 1960b, Phys. Rev. Letters 4, 161.

Sonett, C. P., E. J. Smith and A. R. Sims, 1960c, Space Research I, 921.

Spreiter, J. R. and W. P. Jones, 1963, J. Geophys. Res. 68, 3555.

Van Allen, J. A., 1964, J. Geophys. Res. 69, 1011.

Wilcox, J. W. and N. F. Ness, 1965, GSFC Report X-612-65-302

Williams, D. F. and G. D. Mead, 1965, J. Geophys. Res 70, 3017

Wolfe, J. W., R. W. Silva and M. Myers, 1965, Space Research VI, to appear.

List of Figures

6. Particle and magnetic field measurements with Explorer XII for the inbound pass on September 13, 1961. These data illustrate the termination of the geomagnetic field at a geocentric distance of 52, 200 Km (≈8.2 R_e) and the flux of electrons between 1-10 Kev beyond forming the quasi-thermalized solar plasma (Freeman, Van Allen and Cahill,1963).
7. Illustration of the solar-ecliptic coordinate system employed to study the statistics and character of the magnetic fields in space and the interaction of the solar wind with the geomagnetic field. The X_{se} axis is directed from the Earth to the Sun at all times, the Z_{se} axis is normal to the ecliptic plane and the Y_{se} axis forms a right handed coordinate system.
8. Observed magnetic field results on outbound orbit #1 by the IMP-1 satellite, Nov. 27, 1963. Clearly evident are the magnetosphere boundary at 11.3 R_e and the collisionless shock wave at 16.8 R_e. For a definition of these boundaries see text (Ness et. al., 1965).
9. Representative results from the MIT plasma probe showing measurements of thermalized plasma by IMP-1 during outbound orbit #1. The positions of the boundaries are evidenced by the distinct change to small spin modulation of the observed flux between 11.3 and 16.8 R_e compared to measurements beyond these points (Bridge et.al 1965).

10. Comparison of the IMP-1 rectified boundary crossings with the high speed gas dynamic shock model of Spreiter and Jones (1963). The standoff ratio has been adjusted slightly to match the observations. The predicted shape of the shock is seen to be closely matched by observations. (Ness, 1965b)

11. Magnetic field data from outbound orbit #41, April 30 through May 4, 1964. The apogee of this orbit occurs at a geocentric distance of 31.4 R_e and at a Sun-Earth probe angle of 181^{o}. Throughout most of this time interval the magnetic field is pointed away from the sun but at a geocentric distance of 16 R_e on the inbound pass the magnetic field abruptly reverses direction at the same time that it becomes very small. This spatially limited region is identified as a neutral sheet in the Earth's magnetic tail. (Ness, 1965b)

12. Summary of the hourly average X_{se}-Y_{se} component measurements by the IMP-1 satellite in the Earth's magnetic tail for orbits 1 through 47. Crosses indicate observed traversals of the magnetosphere boundary. Clearly evident is the distortion of the geomagnetic field forming an extended magnetic tail. Abrupt changes in the sense of direction of the tail field correspond to approximately "vertical" traversals of the roughly "horizontal" neutral sheet. (Ness et. al., 1965).

13. Summary illustration of the interpretation of data perpendicular to the plane of the ecliptic illustrating strong day-night asymmetry in the radiation belts and the development of the extended magnetic tail of the Earth. (Ness, 1965b)

14. Interplanetary magnetic field data from January 7, 21 and 22, 1964. $\bar{F}$ is the magnitude of the field in gammas, and θ and ϕ are as defined in Figure 7. The points are shown at 5.46 minute intervals. The range in ϕ labeled "positive" in Figure 15 is shown with a + sign in this figure (field predominatly away from the sun). The range in ϕ labeled "negative" in Figure 15 is indicated with - signs (field predominantly toward the sun). At 2220 UT on Jan 7 the field direction changes to being predominantly toward the sun. (Ness et.al., 1964)

15. Distribution of the measured interplanetary magnetic field direction in the plane of the ecliptic and normal to the ecliptic, averaged over 5.46 minute and 3 hour intervals. The histograms show the field angular distribution per unit solid angle; the dashed circles correspond to an isotropic distribution. The distribution is peaked in directions corresponding to the spiral streaming angle. The angular intervals in which the field is predominantly away from or toward the sun are labeled positive and negative and represented by + and - signs in Figures 14 and 18. The distribution normal to the ecliptic shows that the interplanetary field is predominantly parallel to the ecliptic rather than perpendicular. (Ness and Wilcox, 1964; Ness et.al., 1965)

16. Statistical distribution of the interplanetary magnetic field magnitude for the same data corresponding to that shown in Figure 15. The uniformity of the distribution with an average value of approximately 5 gammas is indicative of average photospheric fields of the sun of a few gauss on the basis of Parker's model of field extension. (Ness et.al. 1965)

17. Auto correlation of the direction of the interplanetary magnetic field as observed by IMP-I (top). This time series yields a significant peak at approximately 27 days. (Ness and Wilcox, 1965) Cross correlation of the IMP-I interplanetary magnetic field data and the photospheric magnetic field for three latitudes illustrating the coherent and statistically significant peak at 4.5 days (bottom) This corresponds to an average velocity of transport of solar lines of flux out to 1 AU of approximately 385 Km/sec. (Ness and Wilcox, 1964).

18. The + and - signs at the circumference of the circles indicate the direction of the measured interplanetary magnetic field during successive 3 hour intervals. A parenthesis around a + or - indicates a time during which the field direction has extended beyond the "allowed regions" shown in Figure 15 for a few hours in a smooth and continuous manner. The inner portion of the figure is a schematic representation of the sector structure of the interplanetary magnetic field that is suggested by these observations. (Ness and Wilcox, 1965)

19. Superposed epoch analysis of the magnitude of the interplanetary magnetic field and the planetary magnetic index Kp as a function of position within the 2/7 sectors shown in Figure 18. The abscissa represents position within the sector, as measured in days, as the sector sweeps past the earth. The ordinate is the average magnitude or average Kp value at the same relative position within the sectors. The results are shown separately for the four sectors with field away from the sun, the three sectors with field toward the sun, and for seven sectors. Wilcox and Ness, 1965)
20. Superposed epoch analysis of the solar wind flux and density as a function of position within the 2/7 sectors as in Figure 19. (Wilcox and Ness, 1965)

SATELLITE	LAUNCH	INCLINATION	LIFETIME (d)
SPUTNIK III	5-15-58	65°	30
PIONEER I	10-11-58	EARTH IMPACT	1
LUNIK I	1-2-59	SOLAR ORBIT	1
EXPLORER VI	8-7-59	47°	61
LUNIK II	9-12-59	LUNAR IMPACT	33.5 HRS.
VANGUARD III	9-18-59	33°	85
PIONEER V	3-11-60	SOLAR ORBIT	50
EXPLORER X	3-25-61	33°	2.2
EXPLORER XII	8-16-61	33°	112
EXPLORER XIV	10-3-62	33°	300
ALOUETTE	9-29-62	80°	STILL TRANS.
EXPLORER XV	10-27-62	18°	90

Figure 1

SATELLITE	LAUNCH	INCLINATION	LIFETIME (d)
ELECTRON-2	1-30-64	61°	90
COSMOS 26	3-18-64	49°	194
ELECTRON-4	7-11-64	61°	?
VELA-3, 4	7-17-64	40°	STILL OPER.
OGO-A	9-5-64	31°	STILL OPER.
EXPLORER-21	10-4-64	34°	150
COSMOS-49	10-24-64	49°	?
1964-83C	12-13-64	89.9°	PART. OPER.
EXPLORER-26	12-21-64	20°	STILL OPER.
VELA-5, 6	7-20-65	40°	STILL OPER.

Figure 2

SATELLITE	INSTRUMENT	RANGE	SENSITIVITY	DISTANCE
SPUTNIK III	TRIAXIAL FLUXGATE	$<6\times10^4$	5%	<1.3
PIONEER I	SEARCH COIL	$<10^3$	1%	3.7–7.0 12.3–14.6
LUNIK I	TRIAXIAL FLUXGATE	<6000	200γ	3–6
EXPLORER VI	SEARCH COIL SOLAR ASPECT	$<2\times10^4$	3%	2–7.5
LUNIK II	TRIAXIAL FLUXGATE	<1500	50γ	3–6
VANGUARD III	PROTON PRECESSION	$10^4-6\times10^4$	4γ	<1.8
PIONEER V	SEARCH COIL	$<10^3$	$0.05-5\gamma$	5–9
EXPLORER X	RB VAPOR FLUXGATES	$30-5\times10^3$ ±50	3γ 0.3γ	1.8–7 6–42.6
EXPLORER XII	TRIAXIAL FLUXGATE	±500	10γ	4–13.5
EXPLORER XIV	TRIAXIAL FLUXGATE	±250	5γ	5–16.5
ALOUETTE	IONOSPHERIC SOUNDING	$<6\times10^4$	0.3%	1.17
EXPLORER XV	TRIAXIAL FLUXGATE	±4000	40γ	1.7–4.0

Figure 3

SATELLITE	INSTRUMENT	RANGE	SENSITIVITY	DISTANCE
ELECTRON-2	TRIAXIAL FLUXGATES (2)	<120 <1200	2γ 20γ	3-11.6
COSMOS-26	PROTON PRECESSION	$<7\times10^4$	$\pm4\gamma$	~1.05
ELECTRON-4	TRIAXIAL FLUXGATES (2)	<240 <1200	?	3-11.4
VELA-3, 4	SEARCH COIL	<27	?	15.7-18.6
OGO-A	RUBIDIUM TRIAXIAL FLUXGATE SEARCH COIL	<500	$\pm3\gamma$	3.8-24.3
EXPLORER-21	RUBIDIUM FLUXGATES	<300 <40	$\pm0.25\gamma$	6-15.9
COSMOS-49	PROTON PRECESSION (2)	$<7\times10^4$	$\pm4\gamma$	~1.05
1964-83C	RUBIDIUM	$<3\times10^4$	$<20\gamma$	1.17
EXPLORER-26	TRIAXIAL FLUXGATE	$<2\times10^3$	$\pm2\gamma$	2.5-5.1
VELA-5,6	SEARCH COIL	<100	?	15.8-18.8

Figure 4

STUDIES OF THE INTERPLANETARY MAGNETIC FIELD

SPACECRAFT (LAUNCH)	LIFETIME (DAYS)	REGION	INSTRUMENT	SENSITIVITY	ACCURACY	COMMENTS
PIONEER V (3-11-60)	50	.9–1.0 AU	SEARCH COIL	$\angle 0.1^{\gamma}$	?	COMPONENT ⊥ TO SPIN AXIS ONLY
EXPLORER X (3-25-61)	2.2	$\angle 47$ R_e	RUBIDIUM, FLUXGATES	$\pm 0.25^{\gamma}$	$\pm 1.0^{\gamma}$	NEVER OUTSIDE EARTHS INFLUENCE
MARINER II (8-26-62)	104	.7–1.0 AU	FLUXGATES	$\pm 0.7^{\gamma}$	?	SPACECRAFT FIELDS, ZEROS UNKNOWN
IMP-1 (11-27-63)	181	$\angle 32$ R_e	RUBIDIUM, FLUXGATES	$\pm .25^{\gamma}$	$\pm .25^{\gamma}$	INITIAL APOGEE TOWARDS SUN
MARINER IV (11-28-64)	STILL OPERATING	1.0–1.5 AU	HELIUM	$\pm 0.7^{\gamma}$	?	SPACECRAFT FIELDS, ZEROS UNKNOWN
IMP-3 (5-29-65)	STILL OPERATING	$\angle 42$ R_e	RUBIDIUM, FLUXGATES	$\pm .25^{\gamma}$	$\pm .25^{\gamma}$	INITIAL APOGEE AT 20 HR. LOCAL TIME

Figure 5

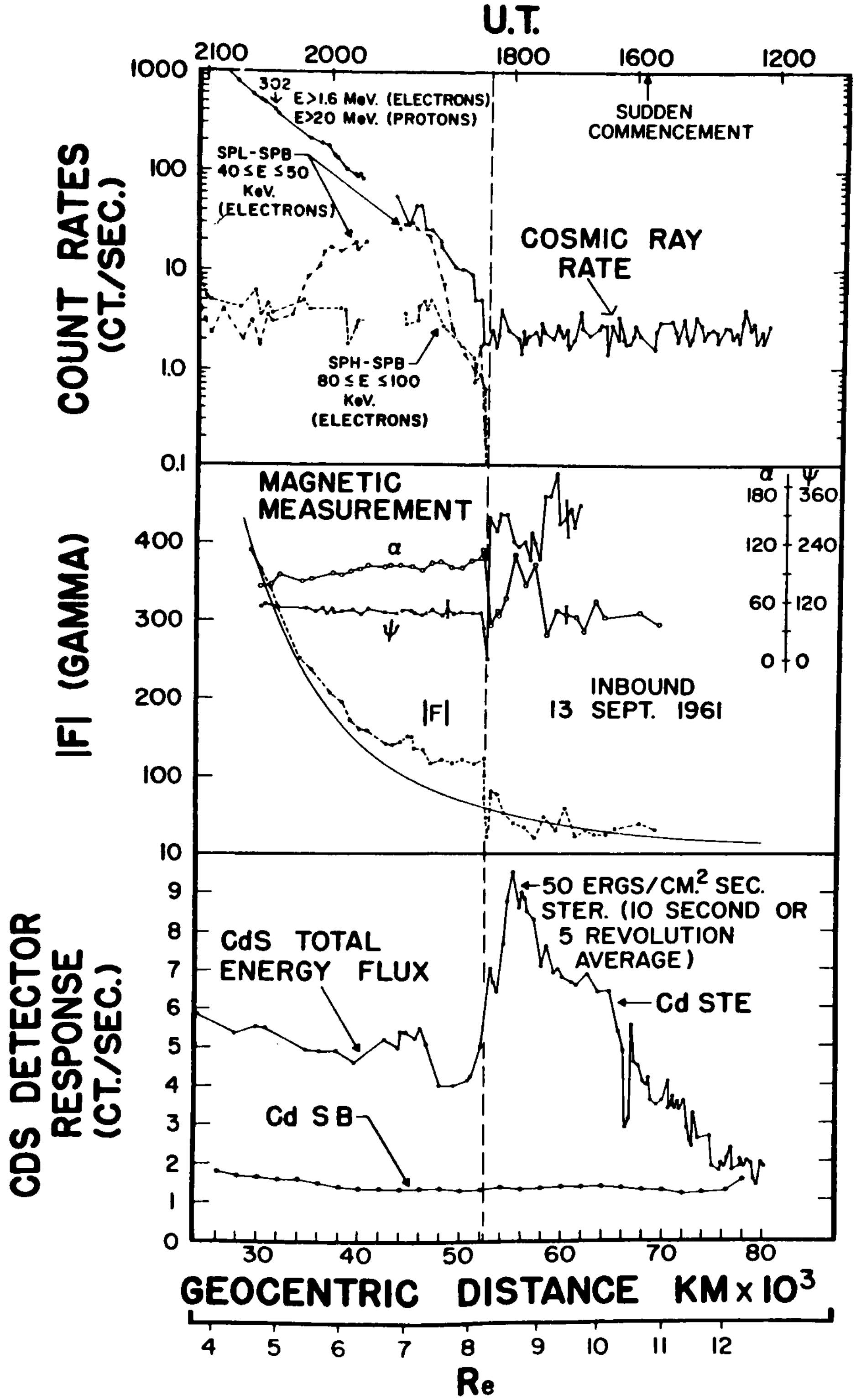
U.T.
2100
2000
1800
1600
1200
1000
100
10
1.0
0.1
COUNT RATES (CT./SEC.)
302
E>1.6 MeV. (ELECTRONS)
E>20 MeV. (PROTONS)
SUDDEN COMMENCEMENT
SPL-SPB
40 ≤ E ≤ 50 KeV. (ELECTRONS)
COSMIC RAY RATE
SPH-SPB
80 ≤ E ≤ 100 KeV. (ELECTRONS)
MAGNETIC MEASUREMENT
|F| (GAMMA)
400
300
200
100
10
α
ψ
|F|
α ψ
180 360
120 240
60 120
0 0
INBOUND
13 SEPT. 1961
CDS DETECTOR RESPONSE (CT./SEC.)
10
9
8
7
6
5
4
3
2
1
0
CdS TOTAL ENERGY FLUX
50 ERGS/CM.2 SEC. STER. (10 SECOND OR 5 REVOLUTION AVERAGE)
Cd STE
Cd SB
30
40
50
60
70
80
GEOCENTRIC DISTANCE KM x 10^3
4
5
6
7
8
9
10
11
12
Re

Figure 6

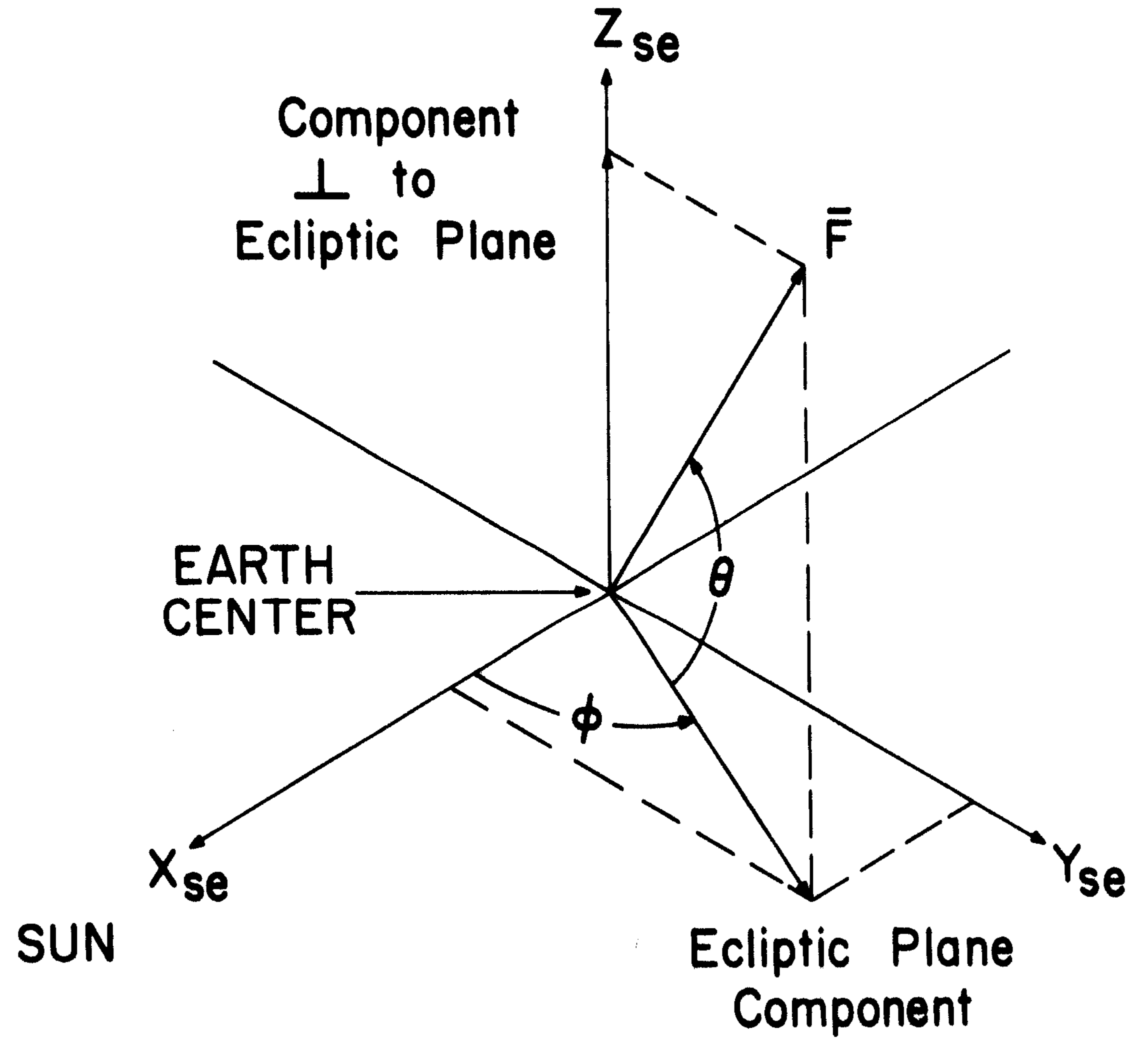

SOLAR ECLIPTIC COORDINATES

Figure 7

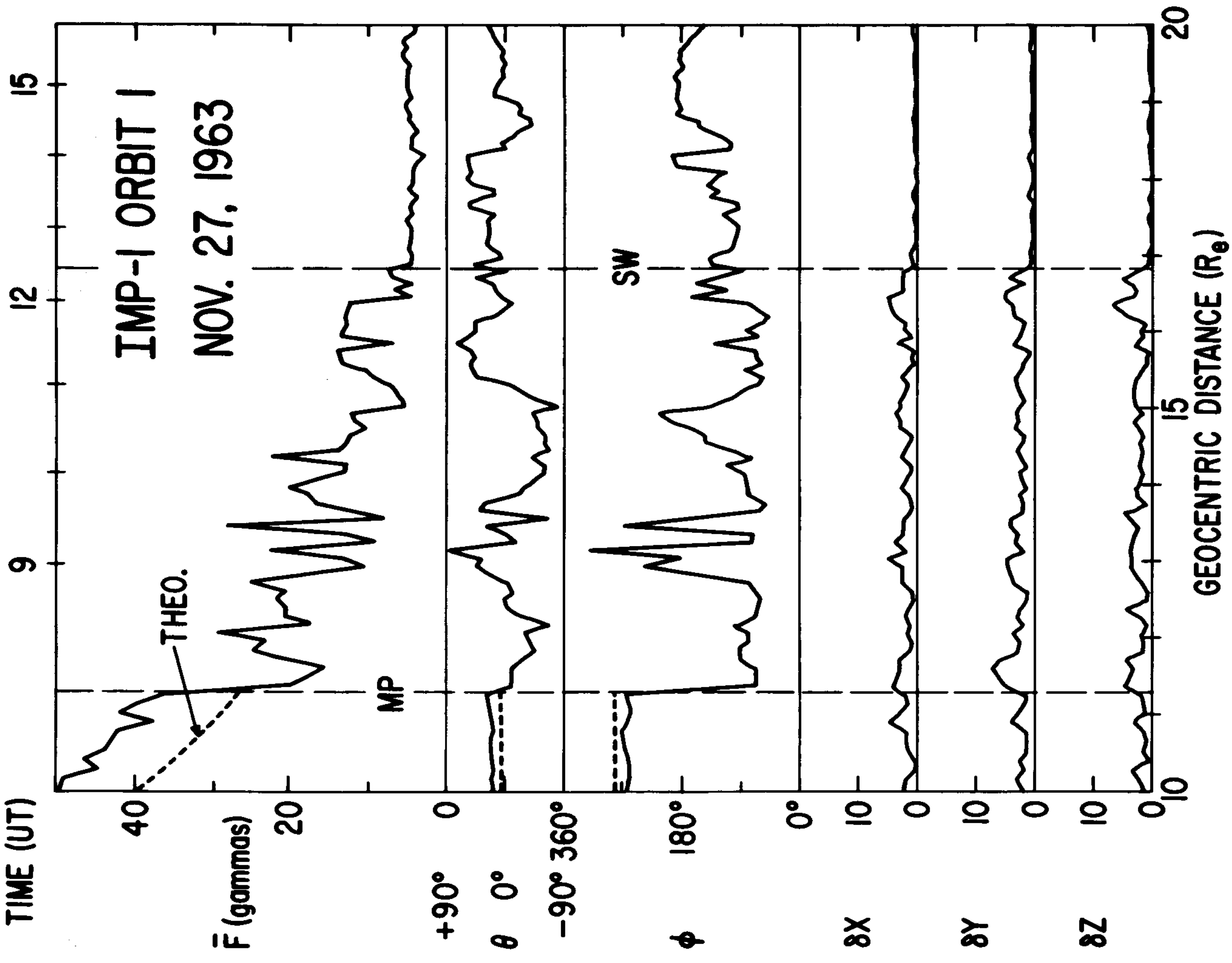

IMP-1 ORBIT I
NOV. 27, 1963
TIME (UT)
9
12
15
$\bar{F}$ (gammas)
40
20
0
THEO.
MP
SW
+90°
θ 0°
-90° 360°
φ
180°
0°
δX
δY
δZ
10
0
GEOCENTRIC DISTANCE (R_e)
10
15
20

Figure 8

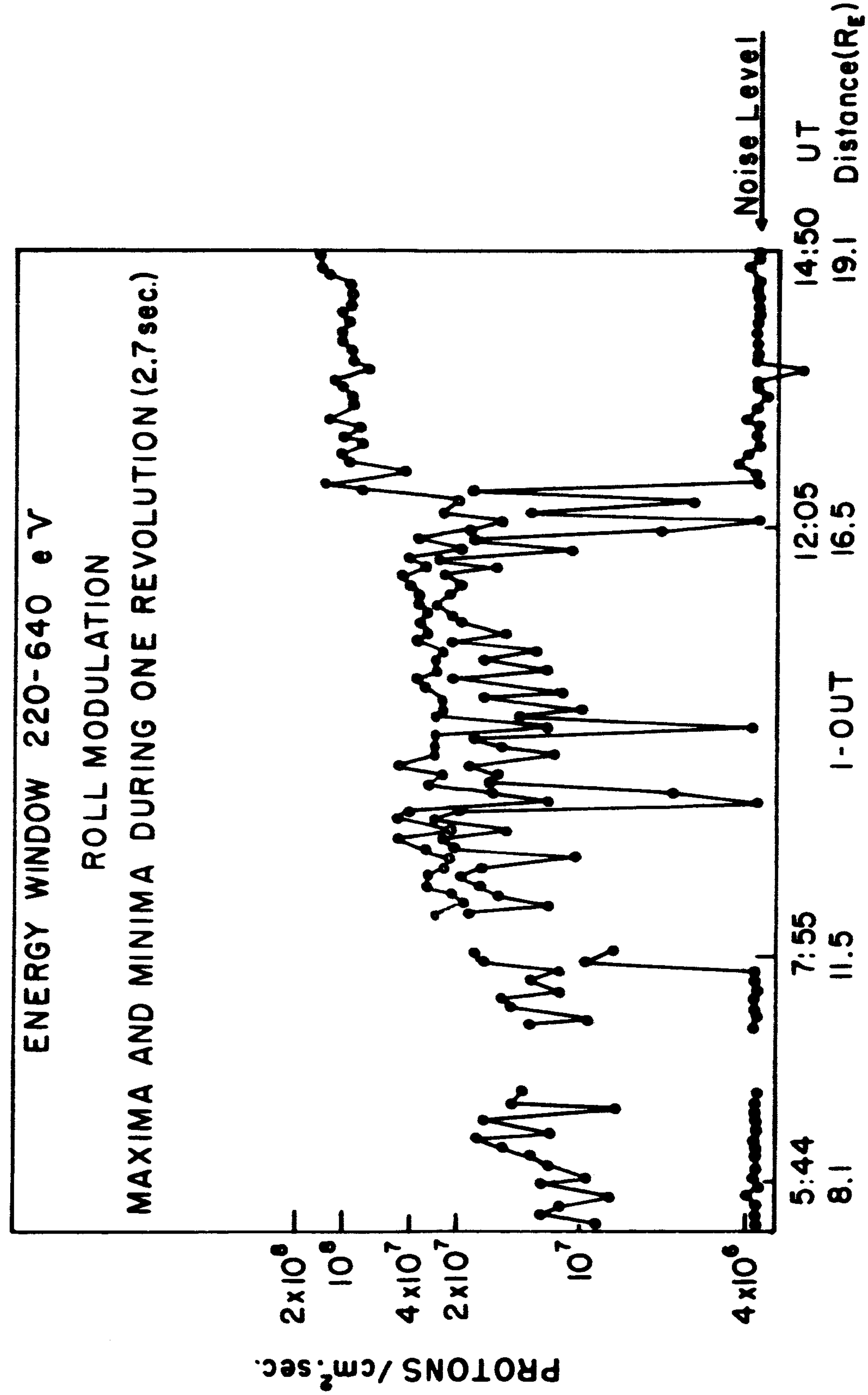

ENERGY WINDOW 220-640 eV
ROLL MODULATION
MAXIMA AND MINIMA DURING ONE REVOLUTION (2.7 sec.)
PROTONS/cm².sec.
2x10⁸
10⁸
4x10⁷
2x10⁷
10⁷
4x10⁶
5:44
8.1
7:55
11.5
12:05
16.5
14:50
19.1
UT
Distance(R_E)
Noise Level
I-OUT
IMP I- 1st PASS OUTBOUND (NOV.27th, 1963)

Figure 9

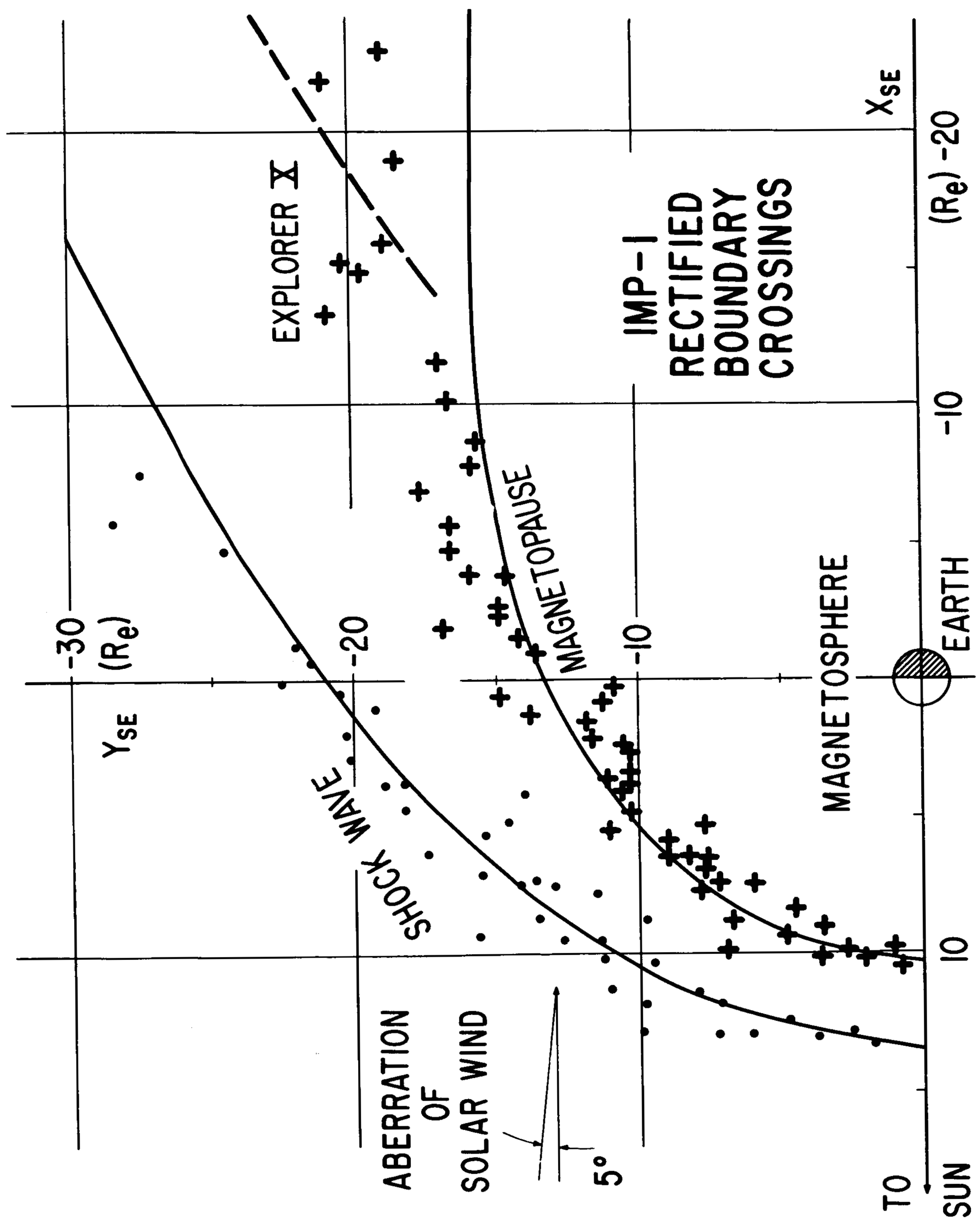

EXPLORER X
IMP-I
RECTIFIED
BOUNDARY
CROSSINGS
MAGNETOPAUSE
MAGNETOSPHERE
EARTH
SHOCK WAVE
ABERRATION
OF
SOLAR WIND
5°
TO
SUN
X_{SE}
(R_e) -20
-10
10
Y_{SE}
-30
(R_e)
-20
-10

Figure 10

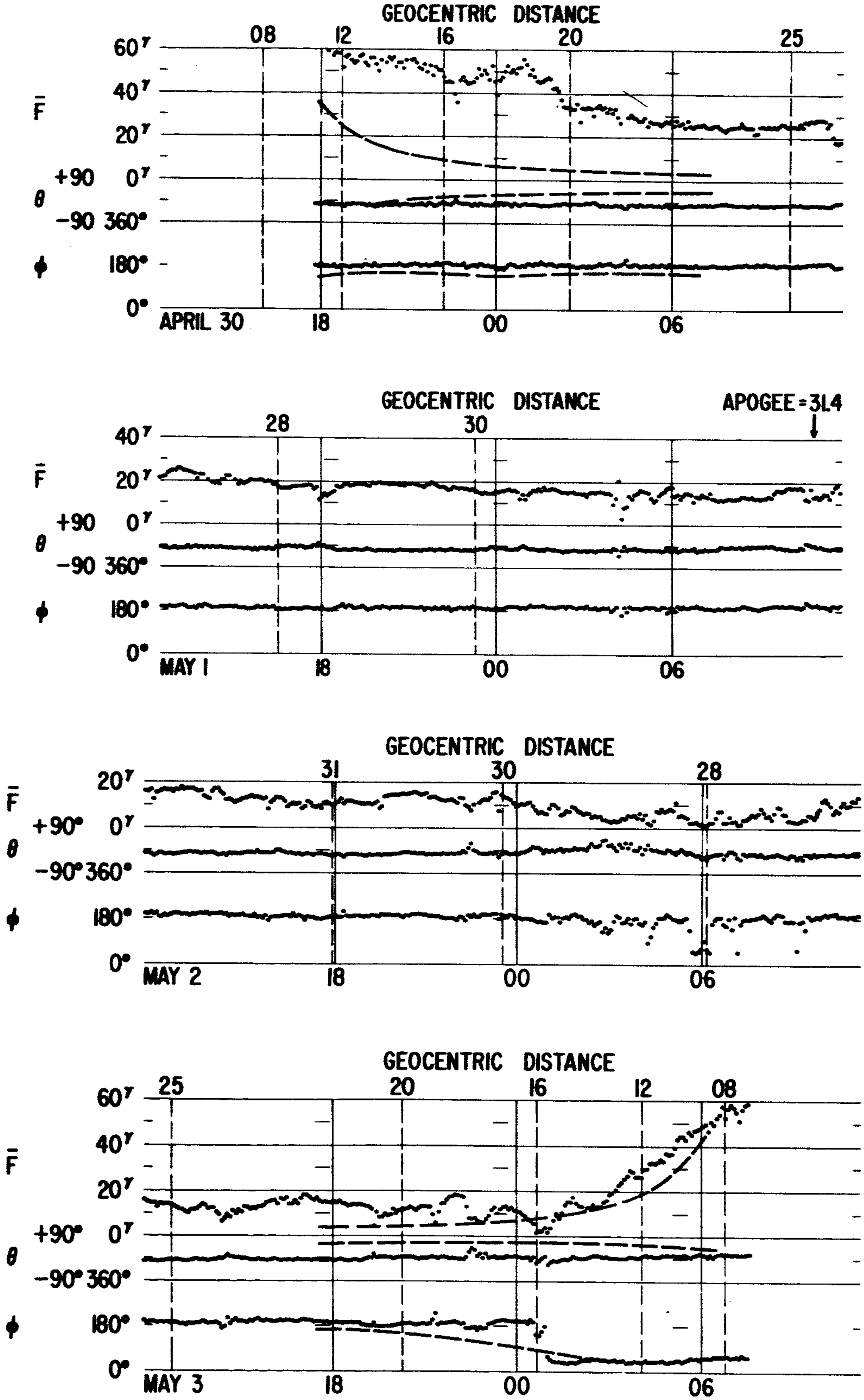

ORBIT NO. 41 IMP-1 1964

Figure 11

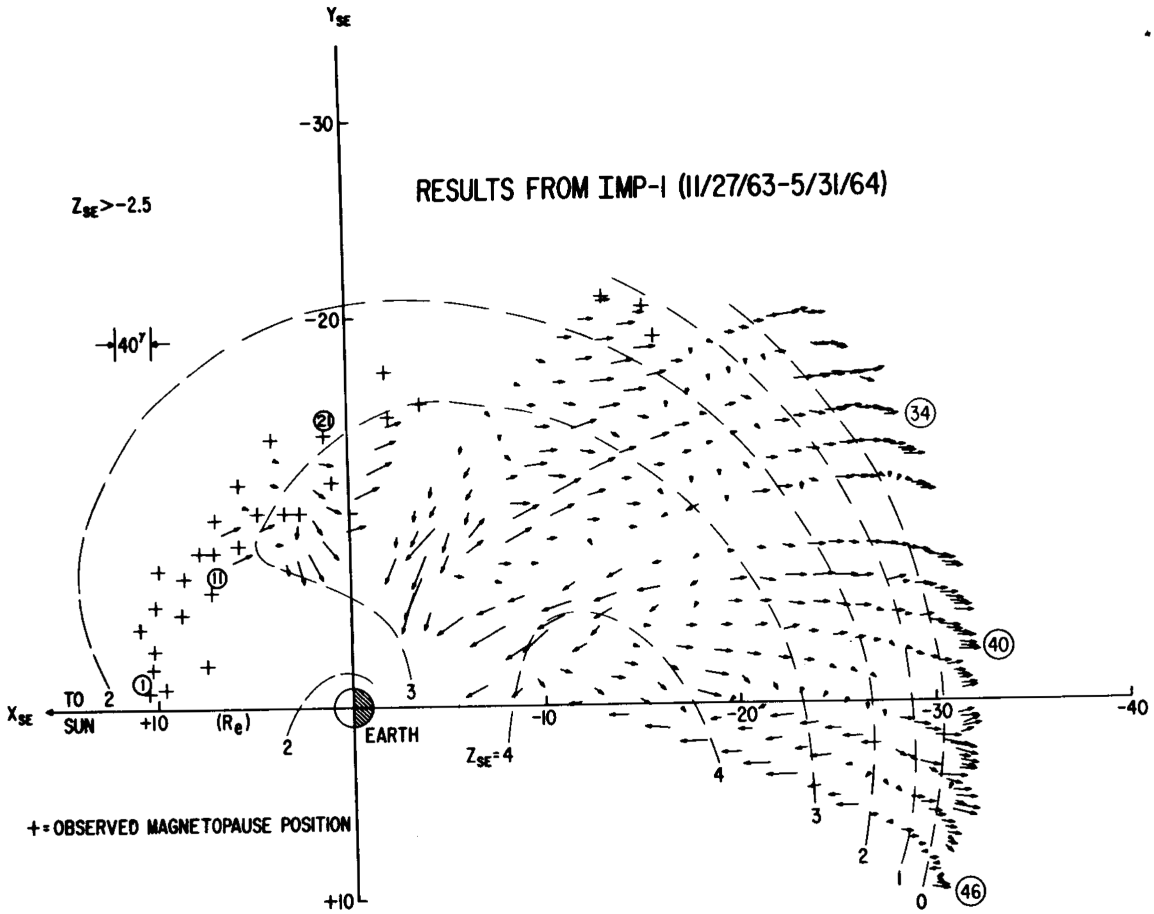
RESULTS FROM IMP-I (11/27/63-5/31/64)
Y_{SE}
$Z_{SE}>-2.5$
40γ
X_{SE}
TO SUN
+10
(R_e)
EARTH
$Z_{SE}=4$
-10
-20
-30
-40
+10
34
40
46
21
11
1
+ = OBSERVED MAGNETOPAUSE POSITION

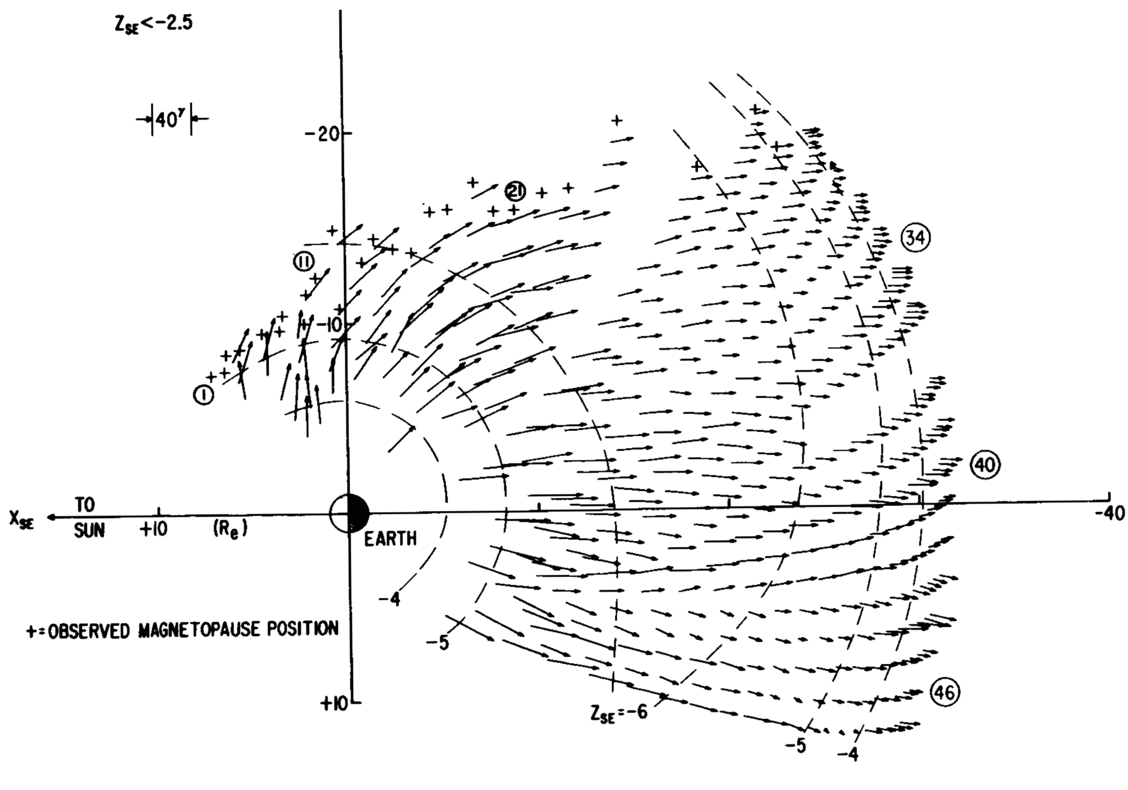
$Z_{SE}<-2.5$
40γ
-20
-10
X_{SE}
TO SUN
+10
(R_e)
EARTH
-40
+10
34
40
46
21
11
1
$Z_{SE}=-6$
+ = OBSERVED MAGNETOPAUSE POSITION

Figure 12

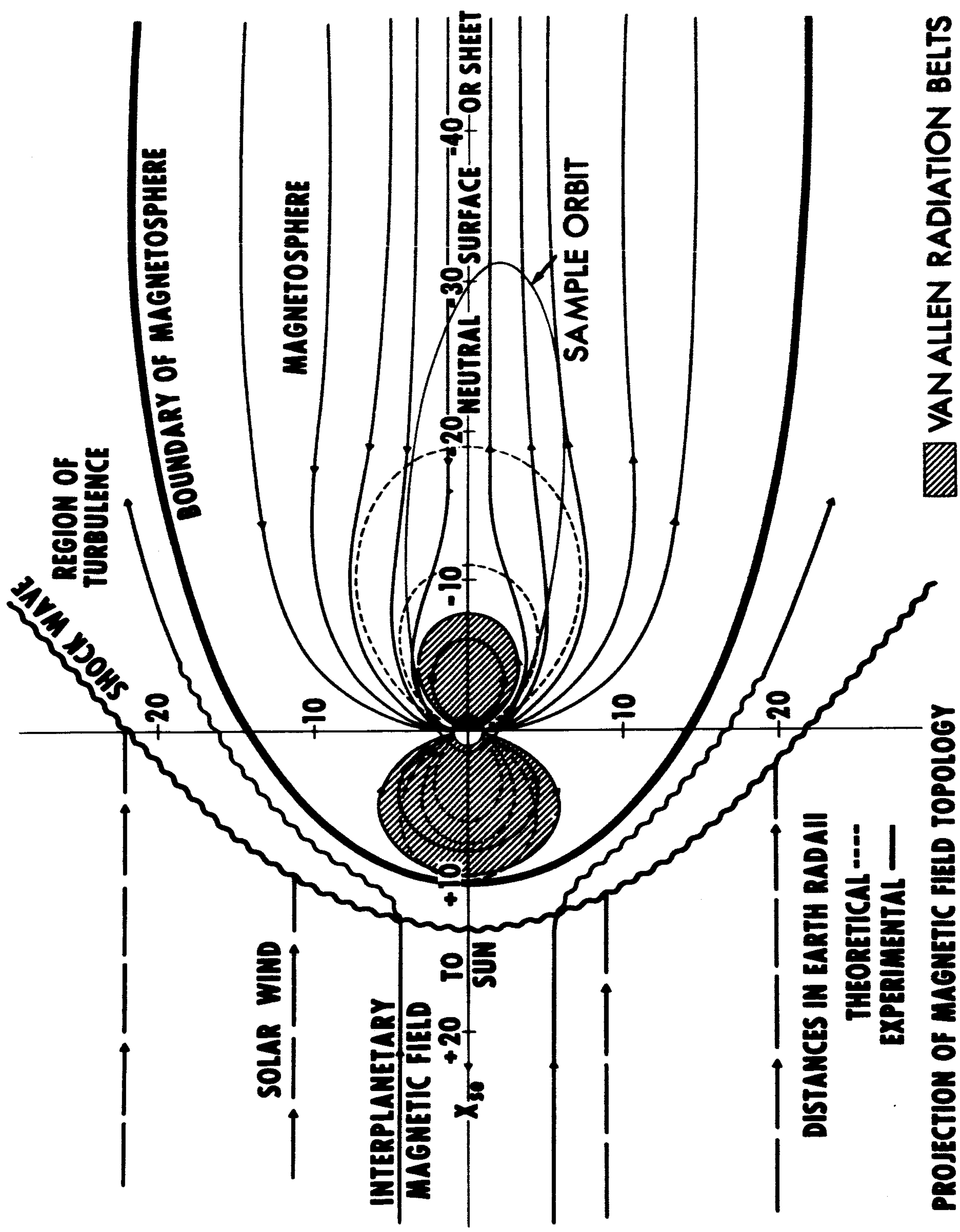
SHOCK WAVE
REGION OF TURBULENCE
BOUNDARY OF MAGNETOSPHERE
MAGNETOSPHERE
NEUTRAL SURFACE OR SHEET
SAMPLE ORBIT
VAN ALLEN RADIATION BELTS
SOLAR WIND
INTERPLANETARY MAGNETIC FIELD
TO SUN
X_{se}
DISTANCES IN EARTH RADAII
THEORETICAL ----
EXPERIMENTAL ——
PROJECTION OF MAGNETIC FIELD TOPOLOGY
ON NOON MIDNIGHT MERIDIAN PLANE

Figure 13

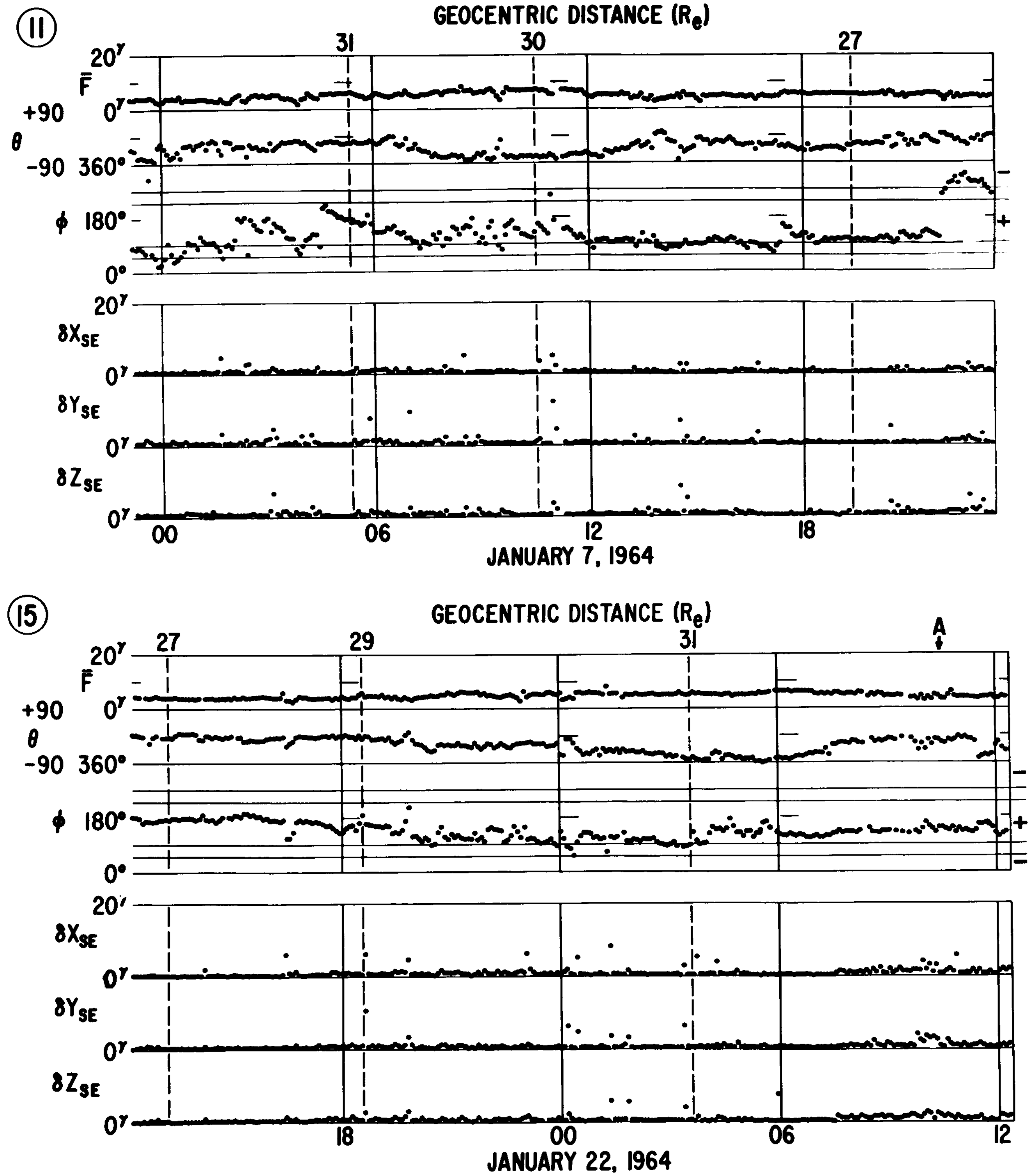

11
GEOCENTRIC DISTANCE (R_e)
31
30
27
20^γ
$\bar{F}$
+90
0^γ
θ
-90
360°
ϕ
180°
0°
20^γ
δX_{SE}
0^γ
δY_{SE}
0^γ
δZ_{SE}
0^γ
00
06
12
18
JANUARY 7, 1964
15
GEOCENTRIC DISTANCE (R_e)
27
29
31
A
20^γ
$\bar{F}$
+90
0^γ
θ
-90
360°
ϕ
180°
0°
20^γ
δX_{SE}
0^γ
δY_{SE}
0^γ
δZ_{SE}
0^γ
18
00
06
12
JANUARY 22, 1964

Figure 14

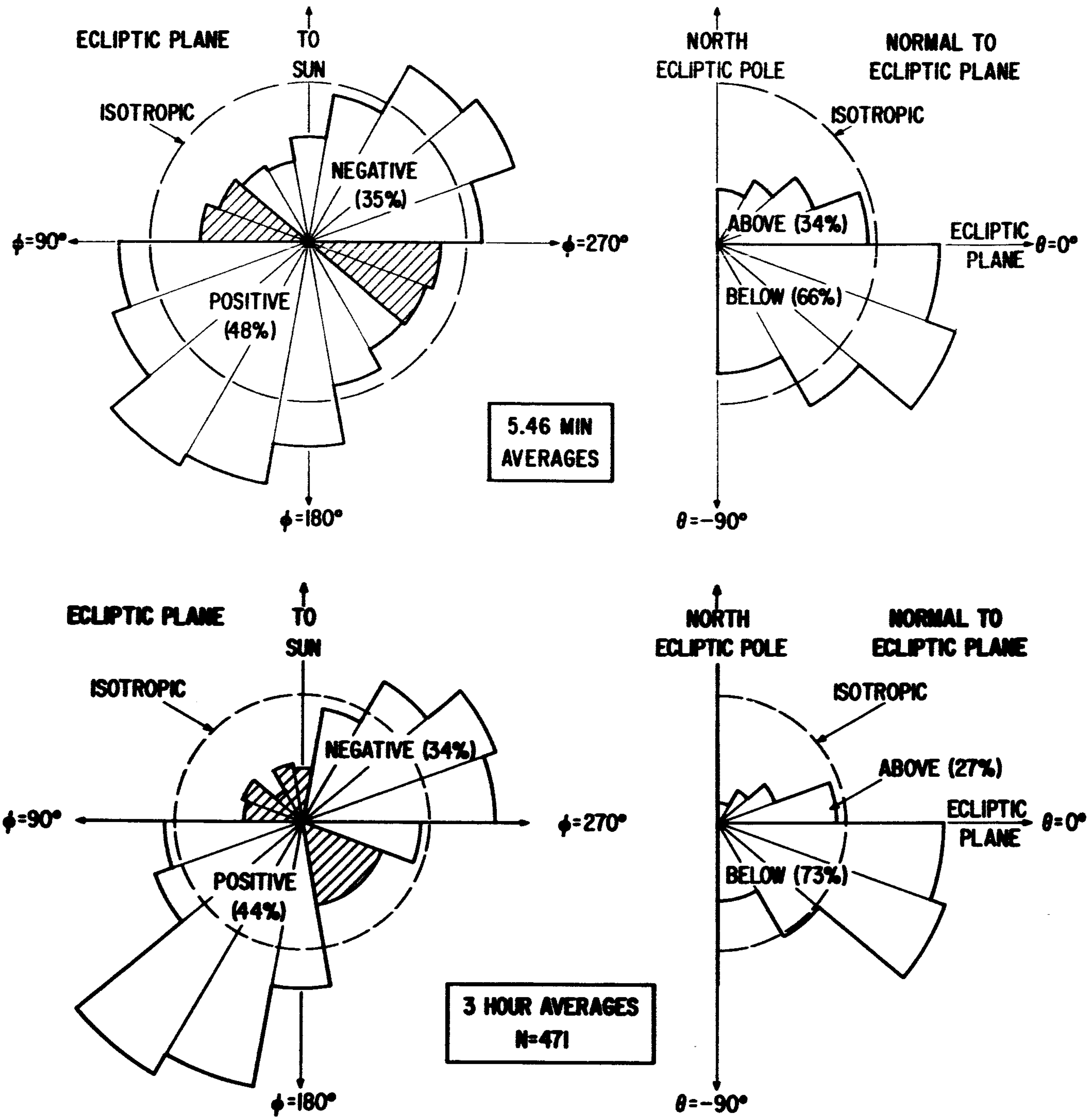

DISTRIBUTION OF INTERPLANETARY MAGNETIC FIELD DIRECTION

Figure 15

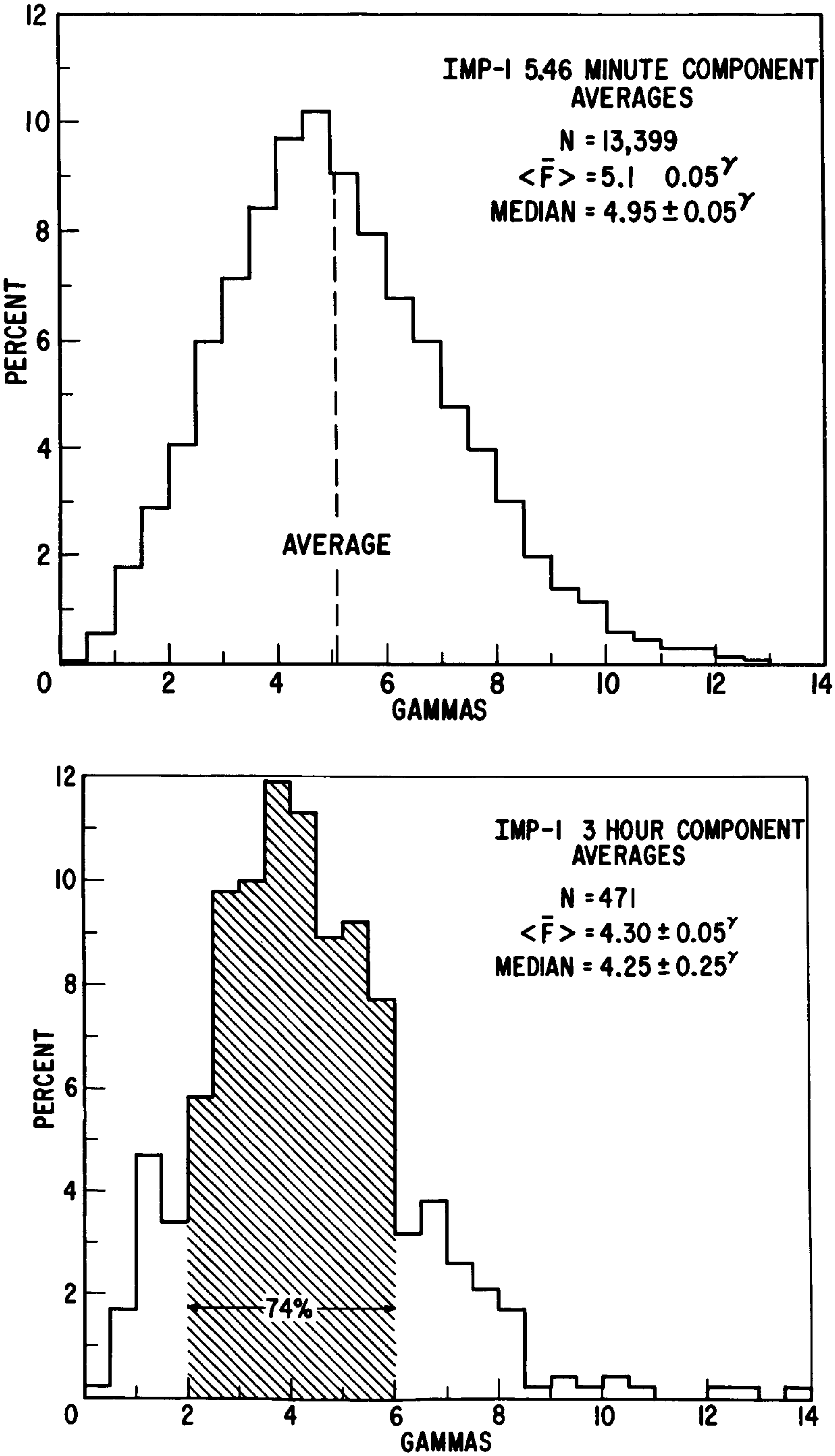

IMP-1 5.46 MINUTE COMPONENT AVERAGES
N = 13,399
<F̄> = 5.1 0.05γ
MEDIAN = 4.95 ± 0.05γ
AVERAGE
PERCENT
GAMMAS
IMP-1 3 HOUR COMPONENT AVERAGES
N = 471
<F̄> = 4.30 ± 0.05γ
MEDIAN = 4.25 ± 0.25γ
74%
PERCENT
GAMMAS

Figure 16

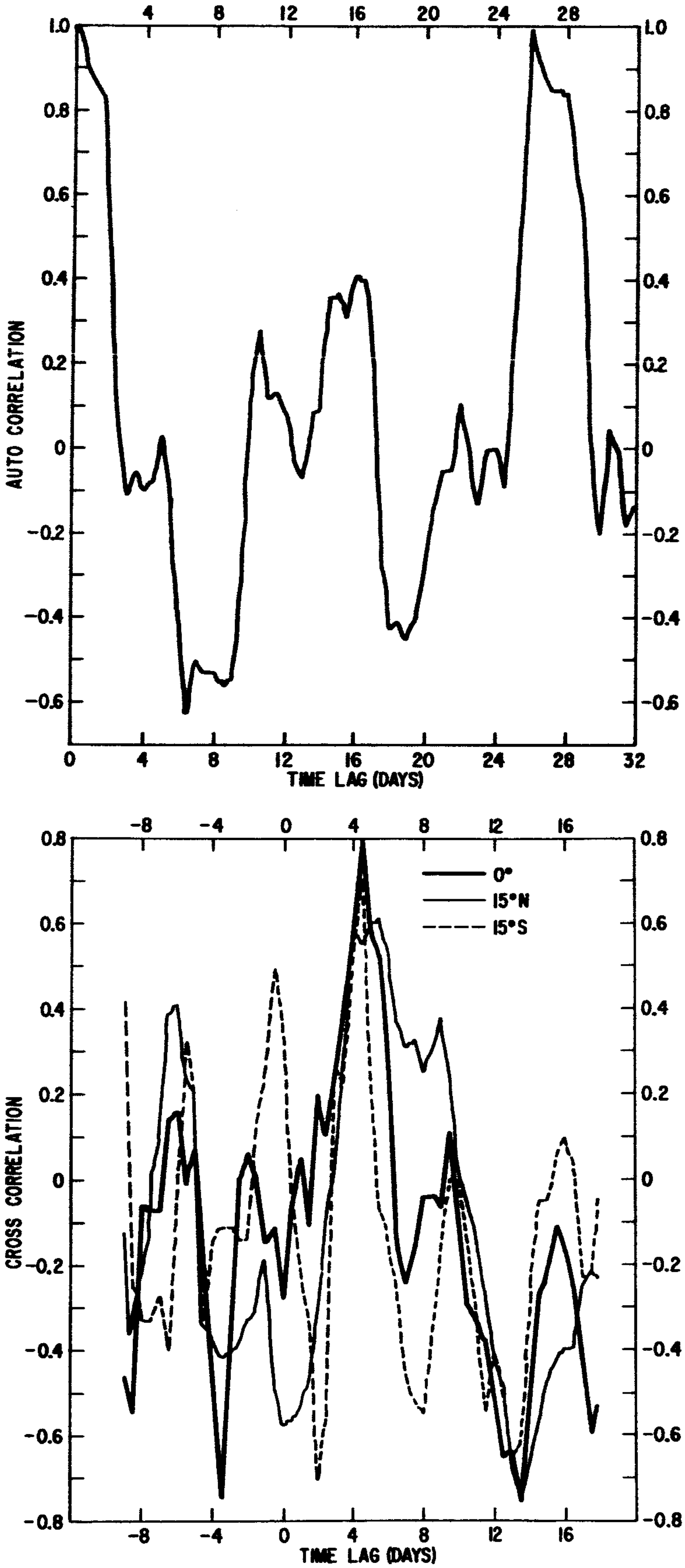
AUTO CORRELATION
TIME LAG (DAYS)
CROSS CORRELATION
0°
15°N
15°S
TIME LAG (DAYS)

Figure 17

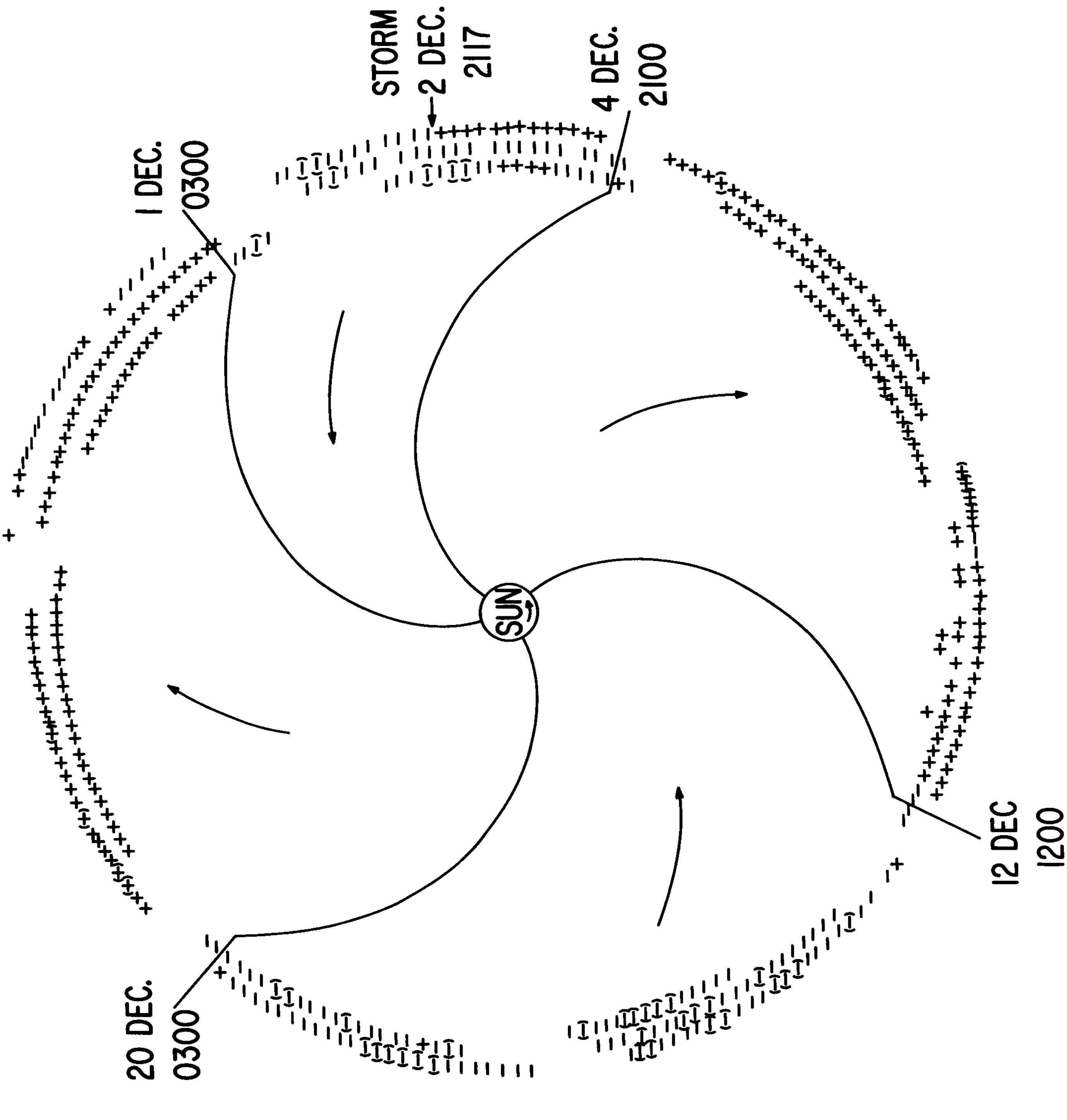
STORM
2 DEC.
2117
4 DEC.
2100
1 DEC.
0300
SUN
12 DEC
1200
20 DEC.
0300

Figure 18

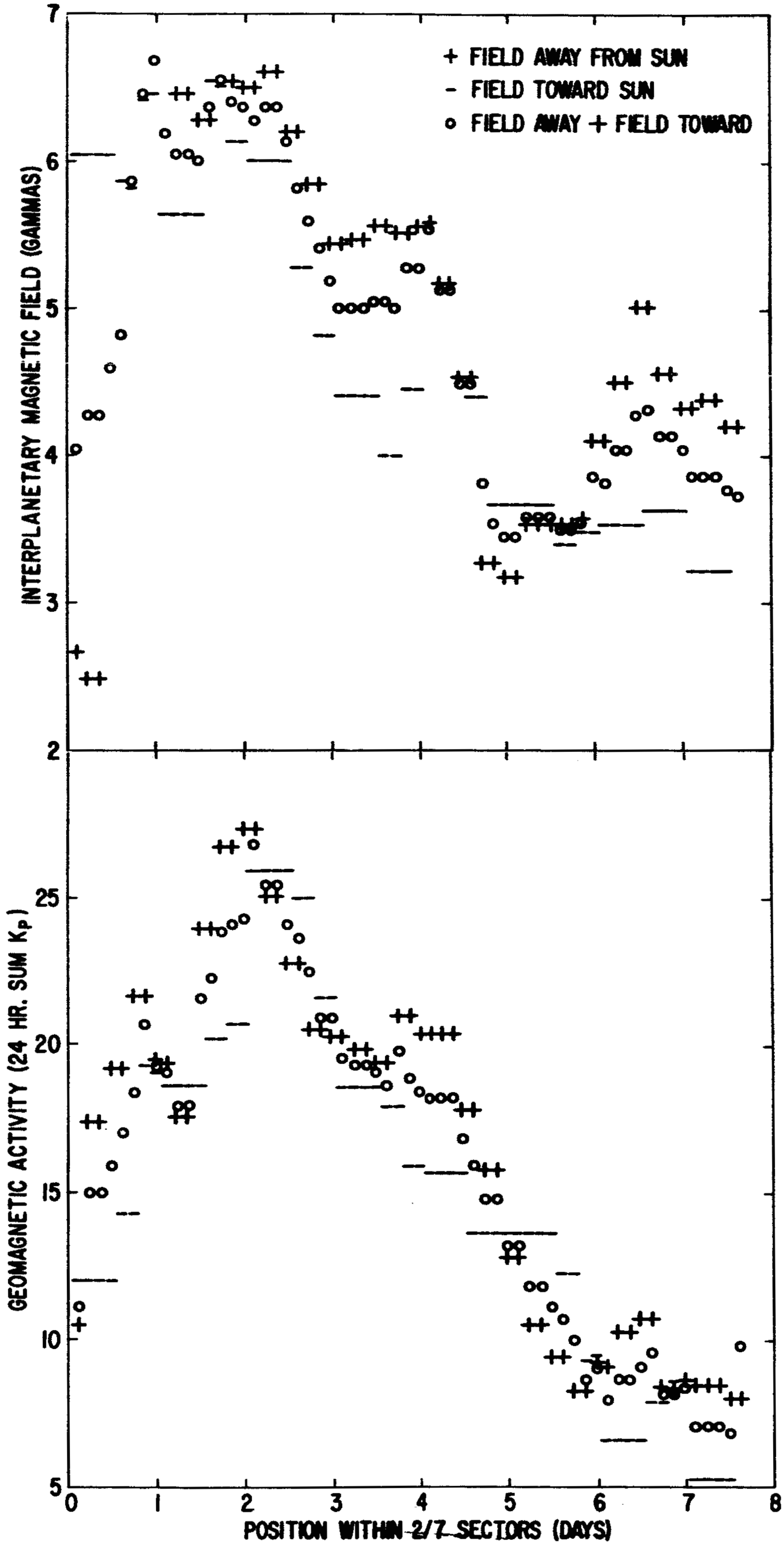
+ FIELD AWAY FROM SUN
- FIELD TOWARD SUN
o FIELD AWAY + FIELD TOWARD
INTERPLANETARY MAGNETIC FIELD (GAMMAS)
GEOMAGNETIC ACTIVITY (24 HR. SUM K_p)
POSITION WITHIN 2/7 SECTORS (DAYS)

Figure 19

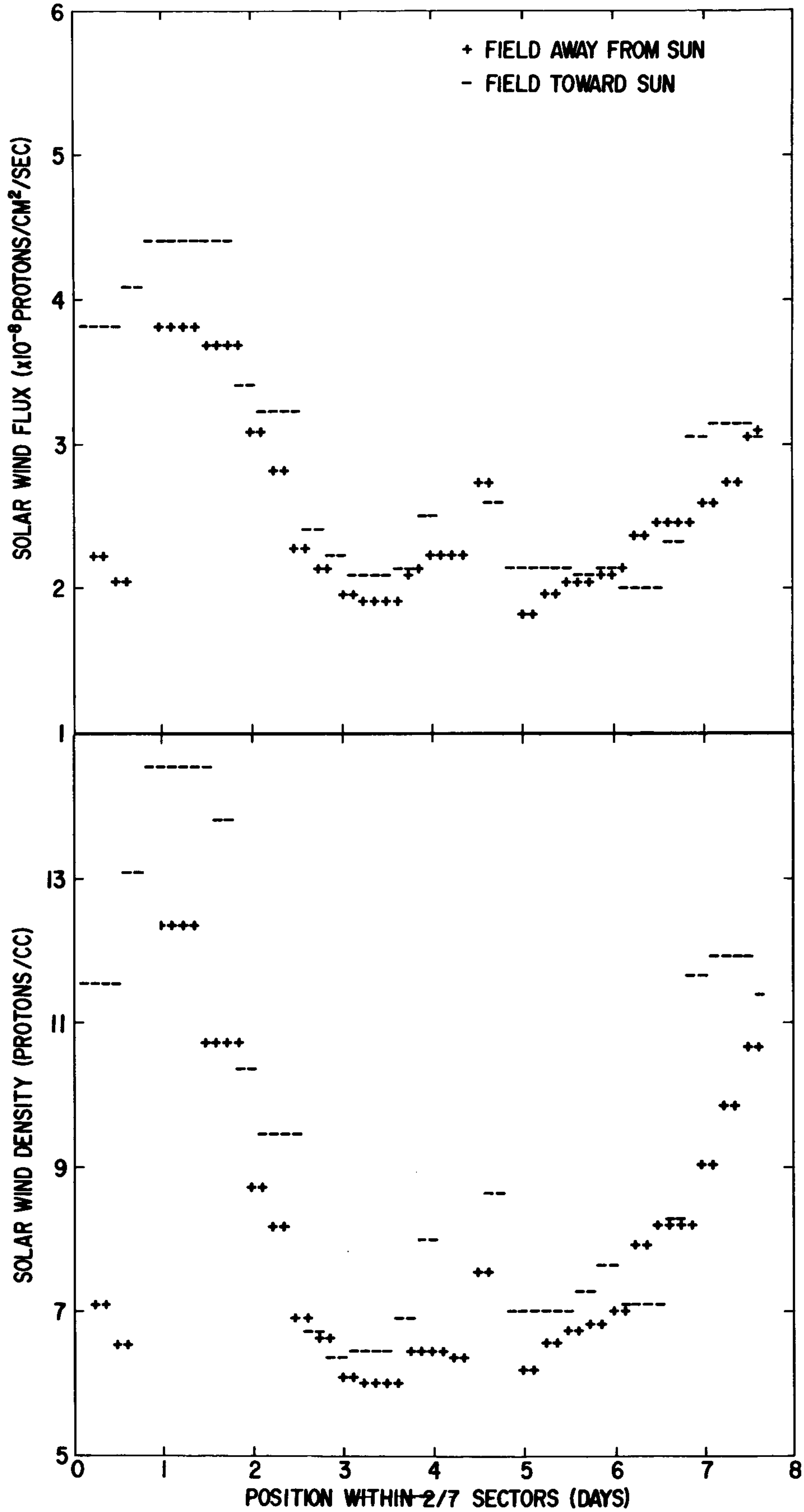

+ FIELD AWAY FROM SUN
− FIELD TOWARD SUN
SOLAR WIND FLUX (x10⁻⁸ PROTONS/CM²/SEC)
SOLAR WIND DENSITY (PROTONS/CC)
POSITION WITHIN 2/7 SECTORS (DAYS)
6
5
4
3
2
1
13
11
9
7
5
0
1
2
3
4
5
6
7
8

Figure 20